Determining Bishop's parameter χ based on pore size distribution

Geng Niu, Yu-Jun Cui, Jean-Michel Pereira, Longtan Shao, De'an Sun

Determining Bishop's parameter χ based on pore size distribution

Geng Niu[1], Yu-jun Cui[2], Jean-Michel Pereira[2], Longtan Shao[1], De'an Sun[3]

[1]Department of Engineering Mechanics, Dalian University of Technology, 116024 Dalian, Liaoning, China
[2]Navier, Ecole des Ponts, Univ Gustave Eiffel, CNRS, Marne-la-Vallée, France
[3]Department of Civil Engineering, Shanghai University, 200444 Shanghai, China

[*]Corresponding author:

Prof. Yu-Jun CUI
Ecole des Ponts ParisTech
6-8 av. Blaise Pascal, Cité Descartes, Champs-sur-Marne
F-77455 Marne-la-Vallée cedex France
Telephone: +33 1 64 15 35 50
Fax: +33 1 64 15 35 62
E-mail: yujun.cui@enpc.fr

Abstract

Extension of the effective stress concept to unsaturated soils has been a major concern for decades. Recent studies significantly contributed to the understanding of the fundamentals behind Bishop's parameter χ which is generally used to define the effective stress for unsaturated soils. Examination of the recently proposed methods showed that the contribution of suction to effective stress was often overestimated, especially in high suction range. In this study, considering that soil pores with different sizes contribute differently to the overall hydro-mechanical behaviour, a new method to determine Bishop's parameter χ is proposed. The key variable used in this method is the ratio of the change in water volume to the change in macro-pore void volume due to loading at constant suction. Shear strength data for a weakly expansive clay were used for validation. A good agreement was obtained between prediction and measurement, indicating the validity of the proposed method.

Keywords:

constitutive relations; fabric/structure of soils; shear strength; partial saturation; suction

NOTATION

e_{w2}	water ratio caused by change of strain at constant suction
e_{w}^{m}	microscopic water ratio
e^{m}	microscopic void ratio
S_{r}^{e}	effective degree of saturation
S_{r}^{m}	microscopic degree of saturation
S_{r}^{cap}	capillary degree of saturation
S_{r}^{ads}	adsorbed degree of saturation
s_{m}	suction corresponding to the median pore diameter
V_{w1}	water volume governed by suction
α	ratio of the change in incremental water volume caused by the change of strain under constant suction to total pore volume increment
λ	material parameter defining the effective degree of saturation
ξ	standard deviation of the log-transformed pore radius
φ	fitting parameter related to the theoretical degree of saturation due to adsorption at 1 kPa suction
χ	Bishop's effective stress parameter

INTRODUCTION

The definition of stress variables is essential in developing constitutive models for unsaturated soils. There are two approaches for modeling their mechanical behaviour: the effective stress approach (Bishop, 1959) and the two independent state variables approach (Coleman 1962, Fredlund & Morgenstern, 1977). Currently, using two independent stress variables to describe the behavior of unsaturated soils is widely accepted (Cui and Delage, 1996; Wheeler *et al*., 2003; Liu *et al*., 2018). Bishop stress is often considered as one variable in the two independent stresses approach, because it represents a smooth extension of Terzaghi's effective stress (Sheng *et al*., 2004; Pereira *et al*., 2005; Zhou *et al*., 2018). In the Bishop's effective stress concept, the key parameter is χ, as shown in Eq. 1 (Bishop, 1959):

$$\sigma' = \sigma - [\chi u_{\mathrm{w}} + (1-\chi)u_{\mathrm{a}}] \tag{1}$$

where σ' is unsaturated effective stress; σ is total stress; χ is the effective stress parameter (Bishop's parameter); u_{w} and u_{a} are water and air pressures, respectively.

In the past few decades, various criteria were reported for determining χ. In the early contributions (Bishop & Blight, 1963), χ was set equal to degree of saturation S_{r}:

$$\chi = S_{\mathrm{r}} \tag{2}$$

which is the simplest, and most used assumption to date. But several studies showed that this choice significantly overestimates the contribution of suction to effective stress, especially in the high suction range (Sheng *et al*., 2011; Zhou *et al*., 2016). In a later effort, the overestimation was reduced by using an effective degree of saturation (Vanapalli *et al*., 1996). To define this latter, attempts have been made to directly relate χ to the total degree of saturation, such as (Vanapalli *et al*., 1996):

$$\chi = f(S_{\mathrm{r}}) = (S_{\mathrm{r}})^{\lambda} \tag{3}$$

where $\lambda \geq 1$ is a material parameter. For coarse-grained soils, parameter λ is almost equal to unity, while for fine-grained soils λ is larger than unity. Garven & Vanapalli (2006) found that λ is correlated with plasticity index, I_{p}.

Soil water consists in capillary water and adsorbed one. Since adsorbed water is strongly bonded to soil particles (Lu *et al*., 2010; Konrad & Lebeau, 2015; Zhou *et al*., 2016; Gao *et al*., 2018), it does not contribute to the contact stress and thus to the effective stress. Thereby, Zhou *et al*. (2016) related the Bishop's parameter χ to the capillary degree of saturation $S_{\mathrm{r}}^{\mathrm{cap}}$ which is the difference between the total degree of saturation and the adsorbed degree of saturation $S_{\mathrm{r}}^{\mathrm{ads}}$:

$$\chi = S_{\mathrm{r}}^{\mathrm{cap}} = \frac{\mathrm{C}(s) - \varphi\mathrm{C}(s)\mathrm{A}(s)}{1 - \varphi\mathrm{C}(s)\mathrm{A}(s)} \tag{4}$$

$$\text{with } C(\mathrm{s}) = \frac{1}{2}\mathrm{erfc}\left[\frac{\ln(s/s_{\mathrm{m}})}{\sqrt{2}\xi}\right],\ A(\mathrm{s}) = 1 - \frac{\ln(s)}{\ln(s_{\mathrm{d}})}$$

where s is matric suction; φ and ξ are fitting parameters determined by soil water retention curve (SWRC); s_{m} is the suction which corresponds to the median pore diameter; s_{d} is the suction at extreme dry state, assumed equal to 10^6 kPa. However, the lastest investigation showed that using capillary degree of saturation underestimates the contribution of suction to Bishop's effective stress for most soils (Gao *et al*., 2020). It has been well documented that for compacted soils, the microstructure is characterised by two pore populations: i) macro-pores where capillary effects dominate, and ii) micro-pores where the hygroscopic effect dominates (Romero & Vaunat, 2000; Alonso *et al*., 2010). It has been admitted that the contribution of suction to Bishop's effective stress is only related to the water trapped in macro- or inter-aggregate pores (Alonso *et al*., 2010; Zhai *et al*., 2019). This was confirmed by some experimental results which showed that loading and drying paths predominantly influenced the macropores, while micropores remain almost undisturbed (Monroy *et al*., 2010; Mašín, 2013). Therefore, Bishop's parameter χ can be considered as the effective degree of saturation of macro-pores $S_{\mathrm{r}}^{\mathrm{e}}$ (Alonso *et al*., 2010):

$$\chi = S_{\mathrm{r}}^{\mathrm{e}} = \frac{S_{\mathrm{r}} - S_{\mathrm{r}}^{\mathrm{m}}}{1 - S_{\mathrm{r}}^{\mathrm{m}}} \tag{5}$$

where $S_{\mathrm{r}}^{\mathrm{m}}$ the degree of saturation of micro-pores. This method can improve the prediction of effective stress, but still overestimates the contribution of suction in some cases (Sheng *et al*., 2011; Zhai *et al*., 2019).

In this study, a new method for determining χ using the macro-PSD is proposed, which satisfies Houlsby's power equation.

DETERMINING BISHOP'S PARAMETER χ BASED ON MACROPOROSITY

Fig. 1 shows a conceptual sketch of water retention curves at two different void ratios (Vaunat & Casini, 2017). The incremental change in water ratio δe_{w} (path OB) caused either by suction change or mechanical loading can be split into δe_{w1} (path OA) and δe_{w2} (path AB). The change of water content along path OA is caused by the increment of suction at constant volume, while the incremental component of path AB is caused by the change of void ratio under constant suction (net stress effect). This latter can be expressed as a proportion of total volume change (Vaunat & Casini, 2017). The total incremental work input per unit volume in unsaturated soils δw (Houlsby, 1997) can be expressed as:

$$\delta w = -[\sigma - \alpha u_\mathrm{w} - (1-\alpha)u_\mathrm{a}]\frac{\delta V_V}{V} - (u_\mathrm{a} - u_\mathrm{w})\frac{\delta V_\mathrm{w1}}{V}$$

$$= -[\sigma - \alpha u_\mathrm{w} - (1-\alpha)u_\mathrm{a}]\delta\varepsilon_V - (u_\mathrm{a} - u_\mathrm{w})\frac{\delta V_\mathrm{w1}}{V} \quad (6)$$

where σ is the total mean stress; V is the total soil volume; V_V is the volume of voids; δV_w1 is the change of volume occupied by water due to suction; α is the ratio of the increment of volume occupied by water caused by the incremental volumetric strain under constant suction to the pore volume increment. As the first term between brackets in Eq. (6) expresses Bishop's effective stress, Vaunat & Casini (2017) proposed:

$$\chi = \alpha = \frac{\delta V_\mathrm{w2}}{\delta V_\mathrm{V}} = \frac{\delta e_\mathrm{w2}}{\delta e} \quad (7)$$

where δe_w2 is the increment of water ratio caused by the change of volumetric strain under constant suction; δe is the increment of void ratio.

Fig. 2 shows the SWRCs under different void ratios for several soils (Li *et al.*, 2007; Salager *et al.*, 2013; Seiphoori *et al.*, 2014; Gao & Sun, 2017). It appears that in low suction range, the water retention curve is dependent on void ratio. By contrast, in higher suction range, the SWRCs are almost the same (Fig. 3). The separating point corresponds to the delimitation between the range of capillary water in macro-pores and the range of adsorbed water in micro-pores (Romero, 1999). Mašín (2013) also discussed the structure evolution with mechanical loading and assumed that loading (compaction) influenced predominantly the macro-pores, while micro-pores remained untouched (Fig. 3). Thus, as the volume change is mainly due to macro-pores changes, Bishop's parameter χ is solely related to the low suction range (Fig. 3). Thereby, Eq.

(7) is modified as:

$$\chi = \frac{\delta e_{\mathrm{w2}} - \delta e_{\mathrm{w}}^{m}}{\delta e - \delta e^{\mathrm{m}}} \tag{8}$$

where $\delta e_{\mathrm{w}}^{m}$ is the incremental microscopic water ratio; δe^{m} is the incremental microscopic void ratio. In Fig. 3, two SWRCs at different void ratios should be provided and the void ratio of every SWRC should be kept constant in the whole suction range. However, in a SWRC test, the void ratio changes with suction changes. As the pore size distribution (PSD) obtained by Mercury Intrusion Porosimetry (MIP) test can be used to determine the SWRC at a constant void ratio (Zhang *et al.*, 2018), the parameters in Eq. (8) can be obtained using two different PSDs, as illustrated in Fig. 4.

EVALUATION OF THE PROPOSED METHOD THROUGH SHEAR STRENGTH

Bishop & Blight (1963) described the shear strength of unsaturated soils by:

$$\tau_f = c' + [(\sigma_{\mathrm{n}} - u_{\mathrm{a}}) + \chi(u_{\mathrm{a}} - u_{\mathrm{w}})] \tan\theta' \tag{9}$$

where τ_f is the shear strength; c' is the effective cohesion at saturated state; σ_n is the normal stress; θ' is the internal friction angle. Using Eq. 9 and considering triaxial conditions, parameter χ can be back-calculated, as follows:

$$\chi = \frac{\frac{q_{\mathrm{f}} - c'\frac{6\cos\theta'}{3-\sin\theta'}}{M} - \bar{p}}{s} \tag{10}$$

where q_{f} is the deviator stress at failure; M=6 sin ϕ'/(3−sin ϕ') is the slope of critical state line; $\bar{p}$=[σ_1+2σ_3]/3-u_{a} is the net mean stress.

The results from the tests on Nanyang expansive clay were used to validate the proposed method for Bishop's parameter χ determination (Fig. 8). Table 1 summarises the physical property indexes and triaxial shear parameters for this clay. Triaxial shear tests were conducted using an unsaturated triaxial testing apparatus supplied by GDS company. In order to obtain the molded samples only in drying process, all triaxial specimens were prepared by static compaction at initial water content of about 0.215 (suction is about 170 kPa) and initial dry density around 1.25 Mg/m^3. Table 2 gives a summary of the test conditions and stress paths. For tests No.1-3, suction was applied using axis-translation technique in triaxial cell, while for tests No.4 and No.5 the suctions (0.8 and 2.5 MPa, respectively) were applied through controlling the water contents (w=14.8% and w=12.55%, respectively) by referring to the SWRC in drying process. For higher suctions, *i.e.* tests No.6-8, the vapor equilibrium method was employed. When the samples of tests No.4-8 reached the target respective suctions, they were put into triaxial cell for further consolidation and shear tests following the stress and suction paths shown in Figs. 5 (a) and (b). The net confining pressure was 100 kPa, and the suctions were 0.05, 0.2, 0.4, 0.8, 2.5, 3.29, 38 and 368 MPa, respectively. In the triaxial shear tests, q_f and $\bar{p}$ were measured for every suction state and given in Table 3. As illustrated in Fig. 2, when the suction is higher than a specific value, the water retention curve is independent of void ratio. In addition, the modulus of soils with high suction are normally very large and the changes of void during shear tests are thus small. Thereby, shear tests under constant water content are often considered as under constant suction in high suction range (Gao *et al.*, 2019; Zhang *et al.*, 2020). Substitution of q_f, $\bar{p}$, c' θ' and s (see Tables 1, 2 and 3) into Eq. (10)

allows the calculation of Bishop's parameter χ for every suction (or degree of saturation), as illustrated in Fig. 8.

As the void ratio of this sample with 3.29 MPa in shear test is 0.99, the PSD curves of two samples compacted at different void ratios (0.81 and 0.92) at the same constant suction of 3.29 MPa are considered. The results are shown in Fig. 6. According to Lloret *et al*. (2003), the macro- and micro-pores are separated by the point where the PSD becomes independent of loading. For bimodal structure, the diameter at the valley bottom between the two pore size families can be considered as the delimiting diameter between micro- and macro-pores. It appears from Fig. 6 that the PSD curves are not affected by the compaction load when the pore diameter is smaller than 4900 nm. Thereby, this diameter was taken as the boundary between macro- and micro-pores. Eq. (8) can then be applied to determine Bishop's parameter χ using the macro-PSDs. Fig. 7 shows the obtained results. For comparison, the parameters in Table 1 are substituted into Eq. (10), and several other methods are applied including Bishop's method with $\chi = S_r$ (Eq. 2), Vanapalli *et al*.'s method (Eq. 3), Zhou *et al*.'s method (Eq. 4), Alonso *et al*.'s method (Eq. 5), and Vaunat & Casini's method (Eq. 7). Results are included in Fig. 8. It is observed that when the global degree of saturation (Eq. 2) is considered as Bishop's parameter χ, significant overestimation of suction contribution is obtained, in agreement with the observation of Alonso *et al*. (2010) and Zhou *et al*. (2016). In Zhou *et al*.'s method, the capillary water is separated from the adsorbed water. Then the capillary degree of saturation (Eq. 4) is used to determine Bishop's parameter χ. Fig. 7 shows the fitted SWRCs by

Zhou *et al*.' SWRC method (Zhou *et al*., 2016) and the corresponding parameters. The relationship between capillary degree of saturation and degree of saturation is plotted in Fig. 8. It appears that this method underestimates the suction contribution to Bishop's effective stress over a wide suction range. In Alonso *et al*.'s method, S_r^m is the degree of saturation of the micro-pores with diameter smaller than 4900 nm. It was found to be about 20% by calculation based on the PSD in Fig. 6. The effective degree of saturation (Eq. 5) is used to determine χ. It appears that the prediction is improved, but the suction contribution is overestimated. Similarly, Vaunat & Casini's method can improve the prediction in the low suction range as Alonso *et al*.'s method, but remains unsatisfactory in the higher suction range. In particular, a small bump on the curve obtained by Vaunat & Casini's method appears in the range of degree of saturation from 5% to 40%, owing to the contribution of micro-pores to the calculation of χ. In Vanapalli *et al*.'s method, a value of 1.6 was fitted for exponent parameter λ. It is observed that the prediction matches the test data well in the low suction range, but gives higher χ values in higher suction range. Interestingly, the proposed method (Eq. 8) shows a good agreement with the experimental results in the full suction range.

CONCLUSIONS

The hydro-mechanical behavior of unsaturated soils is strongly related to the water distribution in pores. As loading and drying predominantly affect the macro-pores, with the micro-pores remaining almost undisturbed, the pore size below which the PSD curves become independent of loading or drying processes can be considered as the delimiting diameter between macro-and micro-pores. This also implies that the contribution of suction to Bishop's effective stress is only related to the water in macro-pores.

Based on a method proposed by Vaunat & Casini (2017) for Bishop's parameter χ determination, a modified method was proposed considering the contribution of capillary water in macro-pores. Bishop's parameter χ was defined as the ratio of the change in -water volume to the change in macro-pores during a loading process at constant suction. When the degree of saturation of macro-pores is zero, χ becomes zero too. The proposed method was evaluated using experimental shear strength data and compared with different methods reported in literature. It appeared that the proposed method allows good agreement between the prediction and measurement over a wide suction range, as opposed to other methods which either overestimate or underestimate the suction contribution to the effective stress. It is however worth noting that more test results are needed to further validate the proposed method.

ACKNOWLEDGEMENTS

The authors are grateful to the China Scholarship Council (CSC grant No. 201806060075), Ecole des Ponts ParisTech and Guilin University of Technology.

References

Alonso, E. E., Pereira, J. M., Vaunat, J. & Olivella, S. (2010). A microstructurally-based effective stress for unsaturated soils. *Géotechnique* **60**, No. 12, 913-925.

Bishop, A. W. (1959). The principle of effective stress. Tek. Ukebl.**106**, No. 39, 859-863.

Bishop, A. W. & Blight, G. E. (1963). Some aspects of effective stress in saturated and partly saturated soils. *Géotechnique* **13**, No. 3, 177-197.

Coleman J.D.1962. Stress strain relations for partly satured soil. Correspondence, Géotechnique **12**, No. 4, 348-350.

Cui Y. J. & Delage P. (1996). Yielding and plastic behaviour of an unsaturated compacted silt. *Géotechnique* **46**, No. 2, 291-311.

Fredlund, D. G. & Morgenstern, N. R. (1977). Stress state variables for unsaturated soils. *J. Geotech. Geoenviron. Engng* **103** (ASCE 12919).

Gao, Y. & Sun, D. A. (2017). Soil-water retention behavior of compacted soil with different densities over a wide suction range and its prediction. *Comput. Geotech.* **91**, 17-26.

Gao, Y., Sun, D., Zhou, A. & Li, J. (2018). Effect of stress state on soil-water retention and its application on the strength prediction. *Géotech. Lett.* **8**, No. 4, 324-329.

Gao, Y., Sun, D. A., Zhu, Z., & Xu, Y. (2019). Hydromechanical behavior of unsaturated soil with different initial densities over a wide suction range. *Acta Geotech.*, 14(2), 417-428.

Gao, Y., Sun, D. A., Zhou, A., & Li, J. (2020). Predicting Shear Strength of

Unsaturated Soils over Wide Suction Range. Int. J. Geomech. 20, No.2, 04019175.

Garven, E. A. & Vanapalli, S. K. (2006). Evaluation of empirical procedures for predicting the shear strength of unsaturated soils. In Unsaturated Soils 2006 (pp. 2570-2592).

Houlsby, G. T. (1997). The work input to an unsaturated granular material. *Géotechnique* **47**, No. 1, 193-6.

Konrad, J. M. & Lebeau, M. (2015). Capillary-based effective stress formulation for predicting shear strength of unsaturated soils. *Can. Geotech. J.* **52**, No. 12, 2067-2076.

Li, J., Sun, D. A., Sheng, D. C., Sloan, S. & Fredlund, D. G. (2007). Preliminary study on soil water characteristics of Maryland clay. *In Proceedings of the 3rd Asian Conference on Unsaturated Soils*, Nanjing, China, 569-574.

Liu, Y., Wei, C. F., Zhao, C. G., Fang, Q. & Li, J. (2018). Work input for unsaturated soils considering interfacial effects. *Int. J. Numer. Anal Methods in Geomech*. **42**, No. 9, 1078-1094.

Lloret, A., Villar, M. V., Sanchez, M., Gens, A., Pintado, X. & Alonso, E. E. (2003). Mechanical behaviour of heavily compacted bentonite under high suction changes. *Géotechnique* **53**, No. 1, 27-40.

Lu, N., Godt, J. W. & Wu, D. T. (2010). A closed-form equation for effective stress in unsaturated soil. *Water Resour. Res*. **46**, No. 5.

Mašín, D. (2013). Double structure hydromechanical coupling formalism and a model for unsaturated expansive clays. *Engng Geol.* **165**, 73-88.

Monroy, R., Zdravkovic, L. & Ridley, A. (2010). Evolution of microstructure in compacted London Clay during wetting and loading. *Géotechnique* **60**, No. 2, 105-119.

Pereira, J. M., Wong, H., Dubujet, P., & Dangla, P. (2005). Adaptation of existing behaviour models to unsaturated states: application to CJS model. *Int. J. Numer. Anal. Methods Geomech.*, **29**, No. 11, 1127-1155.

Romero Morales, E. E. (1999). Characterisation and thermo-hydro-mechanical behaviour of unsaturated Boom clay: an experimental study. Ph.D. thesis. Universitat Politècnica de Catalunya.

Salager, S., Nuth, M., Ferrari, A. & Laloui, L. (2013). Investigation into water retention behaviour of deformable soils. *Can. Geotech. J.* **50**, No. 2, 200-208.

Seiphoori, A., Ferrari, A. & Laloui, L. (2014). Water retention behaviour and microstructural evolution of MX-80 bentonite during wetting and drying cycles. *Géotechnique* **64**, No. 9, 721-734.

Sheng, D., Sloan, S. W. & Gens, A. (2004). A constitutive model for unsaturated soils: thermomechanical and computational aspects. *Comput. Mech.* **33**, No. 6, 453-465.

Sheng, D., Zhou, A. & Fredlund, D. G. (2011). Shear strength criteria for unsaturated soils. *Geotech. Geol. Eng*. **29**, No. 2, 145-159.

Vanapalli, S. K., Fredlund, D. G., Pufahl, D. E. & Clifton, A. W. (1996). Model for the prediction of shear strength with respect to soil suction. *Can. Geotech. J.* **33**, No. 3, 379-392.

Vaunat, J. & Casini, F. (2017). A procedure for the direct determination of Bishop's chi parameter from changes in pore size distribution. *Géotechnique* **67**, No. 7, 631-636.

Wheeler, S. J., Sharma, R. S. & Buisson, M. S. R. (2003). Coupling of hydraulic hysteresis and stress–strain behaviour in unsaturated soils. *Géotechnique* **53**, No. 1, 41-54.

Zhai, Q. Rahardjo, H., Satyanaga, A., & Dai, G. (2019). Estimation of unsaturated shear strength from soil-water characteristic curve. *Acta Geotech*. **14**, 1977-1990.

Zhang, F., Cui, Y., Zeng, L., Robinet, J. C., Conil, N. & Talandier, J. (2018). Effect of degree of saturation on the unconfined compressive strength of natural stiff clays with consideration of air entry value. *Engng Geol*. **237**, 140-148.

Zhang, J., Niu, G., Li, X. & Sun, D. A. (2020). Hydro-mechanical behavior of expansive soils with different dry densities over a wide suction range. *Acta Geotech.* **15**, No. 1, 265-278.

Zhou, A., Huang, R. & Sheng, D. (2016). Capillary water retention curve and shear strength of unsaturated soils. *Can. Geotech. J*. **53**, No. 6, 974-987.

Zhou, A., Wu, S., Li, J. & Sheng, D. (2018). Including degree of capillary saturation into constitutive modelling of unsaturated soils. *Comput Geotech*. **95**, 82-98.

Table captions.

Table 1 Physical property indexes and shear strength parameters of Nanyang weakly expansive soil

Table 2 Relevant state variables in triaxial tests

Table 3 Stress state at triaxial shear failure

Figure captions.

Fig. 1 Partition of total water volume change into components due to suction and deformation only for a path going from the water retention curve at e to $e+\delta e$ (after Vaunat & Casini, 2017)

Fig. 2. SWRCs under different void ratios over a wide suction range for soils: (a) a clayey silty sand (data from after Salager et al., 2013); (b) MX-80 granular bentonite (data from Seiphoori et al., 2014); (c) Maryland clay (data from Li et al., 2007); (d) Pearl clay (data from Gao & Sun, 2017)

Fig. 3 Sketches of soil-water retention behavior of specimens with different densities over a wide suction range

Fig. 4 PSDs at two different void ratios (compacted at different void ratios at a constant suction)

Fig. 5 Stress and suction paths for tests: (a) tests in the lower suction range; (b) tests in the higher suction range

Fig. 6 The PSD of Nanyang weakly expansive soil and the criterion adopted to discriminate macro- and micro-pores

Fig. 7 Measured SWRC and fitted curves from Zhou et al.' SWRC method (2016) for Nanyang weakly expansive soil

Fig. 8 Comparison of measured Bishop's parameter χ with the predictions obtained by various methods for Nanyang weakly expansive soil

Table 1 Physical property indexes and shear strength parameters of Nanyang weakly expansive soil

Specific gravity	Liquid limit (%)	Plastic limit (%)	Plasticity index	Shrinkage limit (%)	Maximum dry density (g/cm^3)	Optimum water content (%)	Free swelling ratio (%)	Effective cohesion（kPa）	Effective friction angle (°)
2.74	38.8	17.2	21.6	10.5	1.69	18.2	53.8	10.4	20.8

Table 2 Relevant state variables in triaxial tests

Test No.	Molding state			Before triaxial shearing			Suction (MPa)	Control suction method	Net cell pressure (kPa)
	w_0	S_{r0}(%)	e_0	w	S_r(%)	e			
1	21.50	48.45	1.216	24.14	79.13	0.826	0.05	Axis-translation technique	100
2	22.01	50.13	1.203	19.12	52.79	0.982	0.20		
3	21.50	48.97	1.203	17.07	45.30	1.02	0.40		
4	21.64	49.54	1.197	14.80	38.44	1.04	0.80	Air-drying	
5	21.78	49.57	1.204	12.55	35.52	0.957	2.50		
6	21.86	49.95	1.199	11.90	32.53	0.996	3.29	Vapor equilibrium technique	
7	21.72	49.51	1.202	6.60	19.57	0.924	38.0		
8	21.76	49.52	1.204	4.10	12.20	0.907	367.5		

Table 3 Stress state at triaxial shear failure

Test No.	Control suction method	Net cell pressure (kPa)	Deviator stress q_f (kPa)	Net mean stress $\bar{p}$ (kPa)
1	Axis-translation technique	100	140	146
2			210	160
3			280	196
4	Air-drying		320	210
5			600	300
6	Vapor equilibrium technique		660	326
7			1290	550
8			1680	660

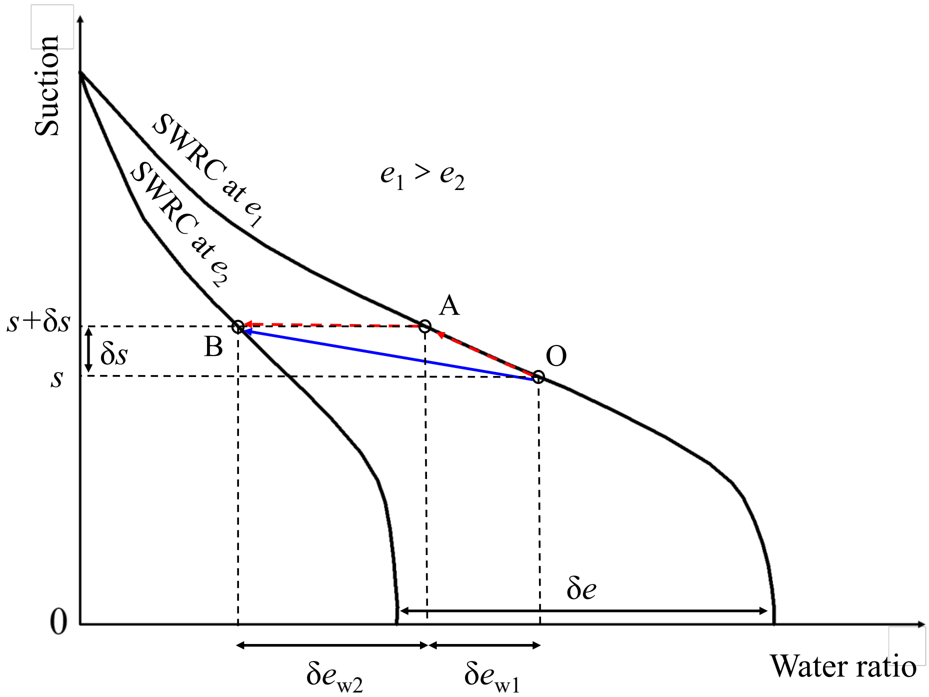

Fig. 1. Partition of total water volume change into components due to suction and deformation only for a path going from the water retention curve at e to $e+\delta e$ (after Vaunat & Casini, 2017)

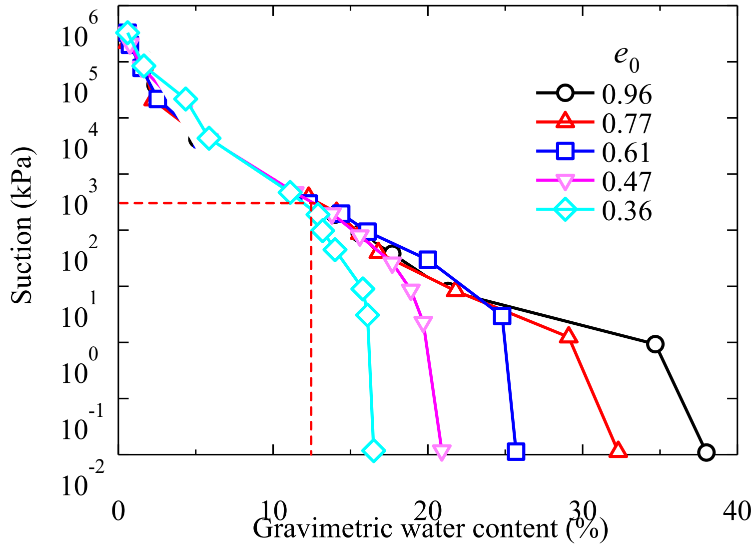

379 (a)

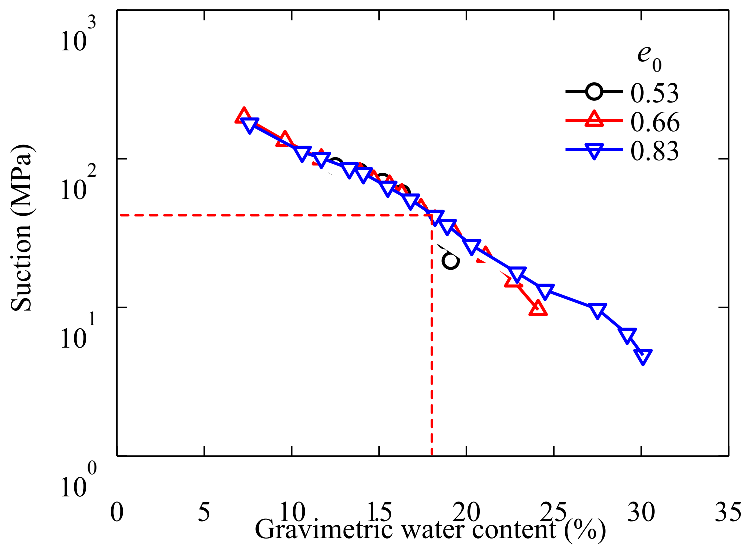

380 (b)

381

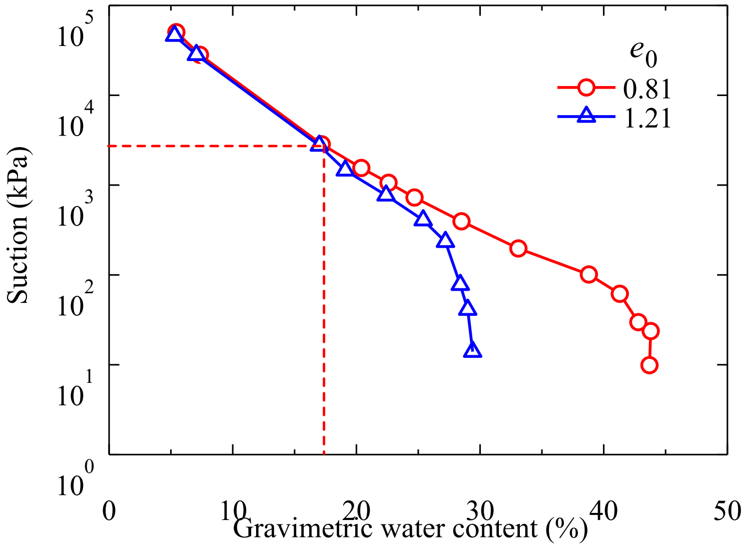

(c)

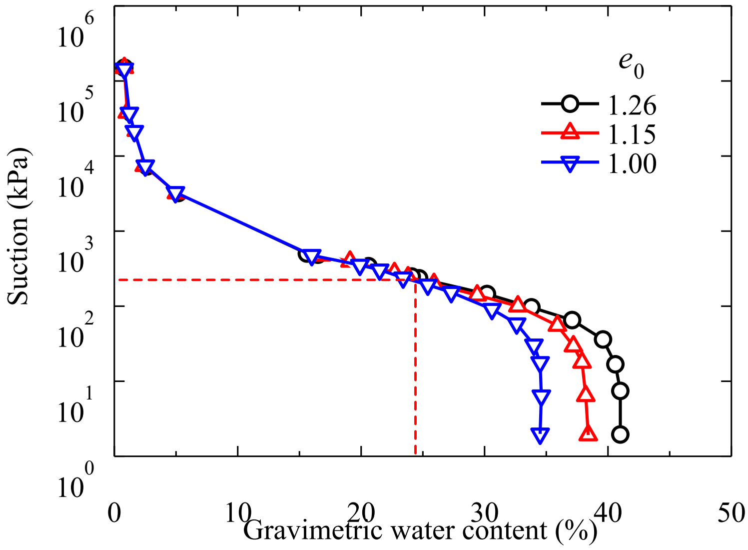

(d)

Fig. 2. SWRCs under different void ratios over a wide suction range for soils: (a) a clayey silty sand (data from after Salager *et al*., 2013); (b) MX-80 granular bentonite (data from Seiphoori *et al*., 2014); (c) Maryland clay (data from Li *et al*., 2007); (d) Pearl clay (data fron Gao & Sun, 2017)

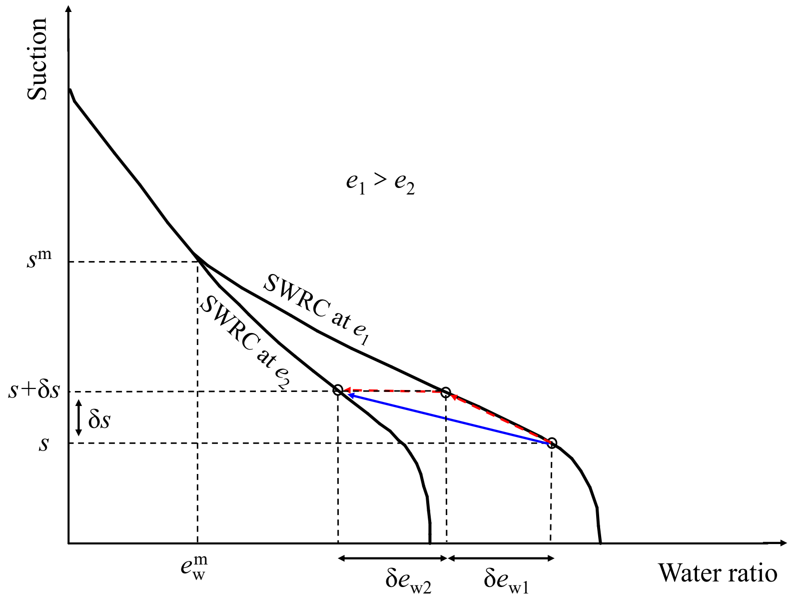

Fig. 3. Sketches of soil-water retention behavior of specimens with different densities over a wide suction range

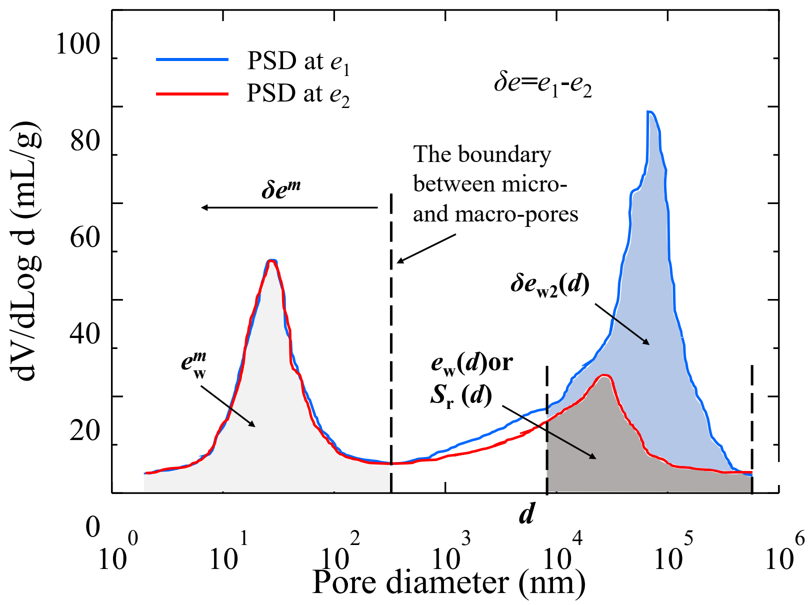

Fig. 4. PSDs at two different void ratios (compacted at different void ratios at a constant suction)

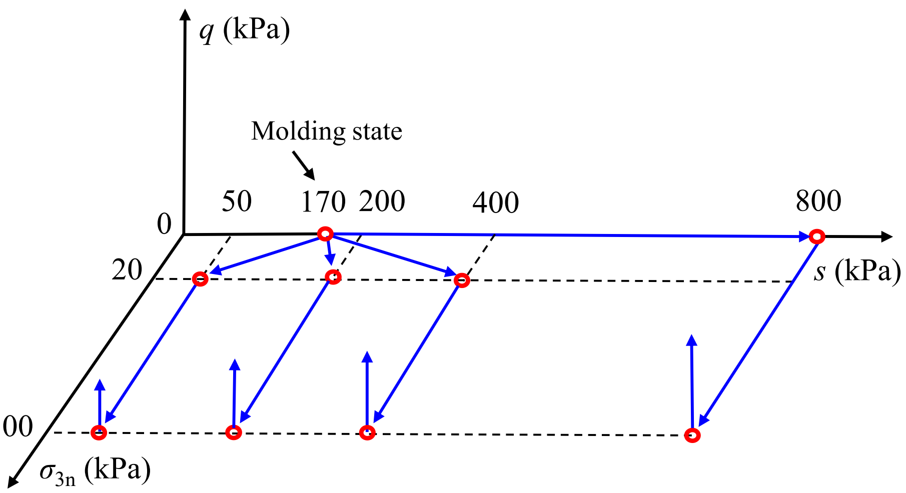

(a)

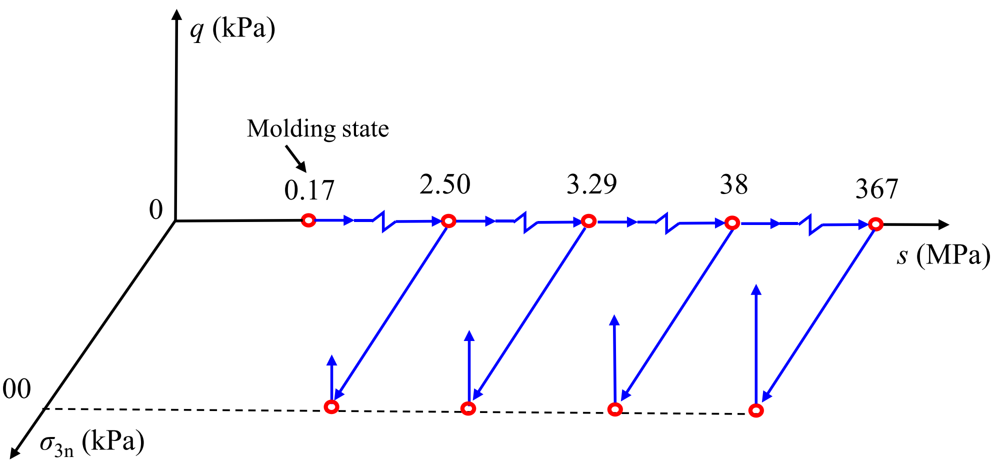

(b)

Fig. 5. Stress and suction paths for tests: (a) tests in the lower suction range; (b) tests in the higher suction range

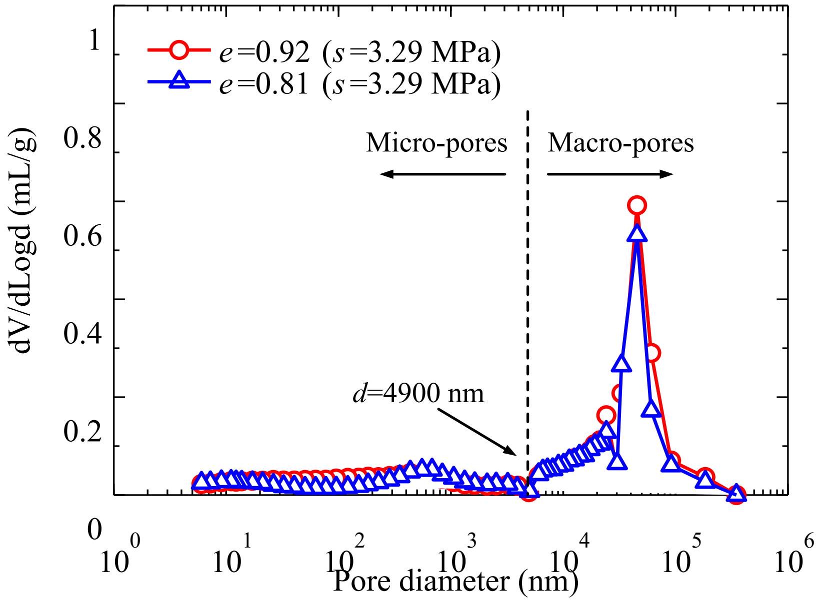

Fig. 6. The PSDs of Nanyang weakly expansive soil and the criterion adopted to discriminate macro- and micro-pores

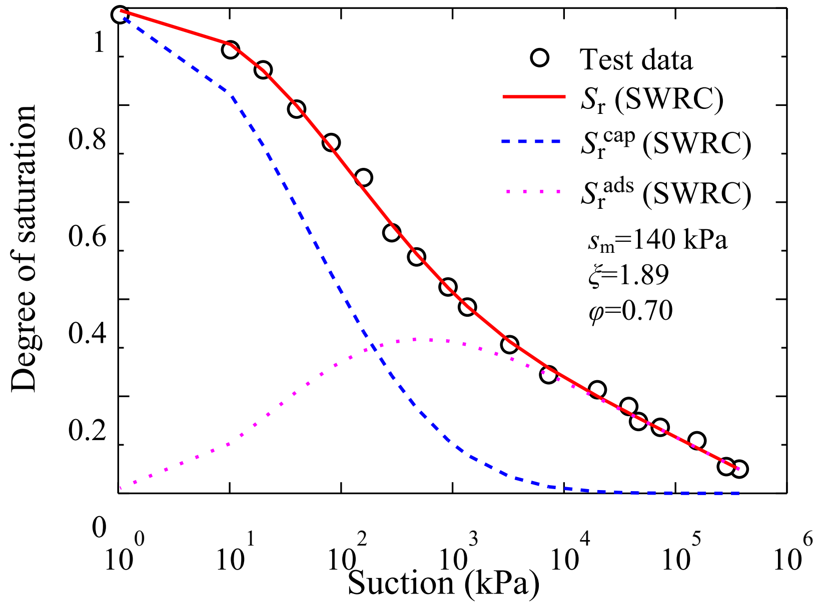

Fig. 7 Measured SWRC and fitted curves from Zhou *et al.*' SWRC method (2016) for Nanyang weakly expansive soil

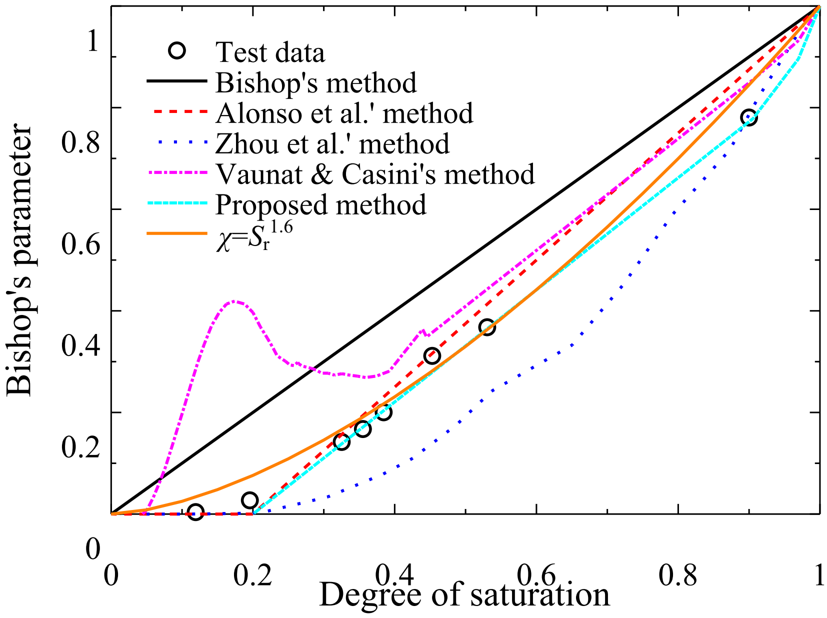

Fig. 8. Comparison of measured Bishop's parameters χ with the predictions obtained by various methods for Nanyang weakly expansive soil